Appendix F

SEM Images

(EBS-14 to EBS-23)

and

(FEBEX SAMPLES)

SEM Images

EBS-14

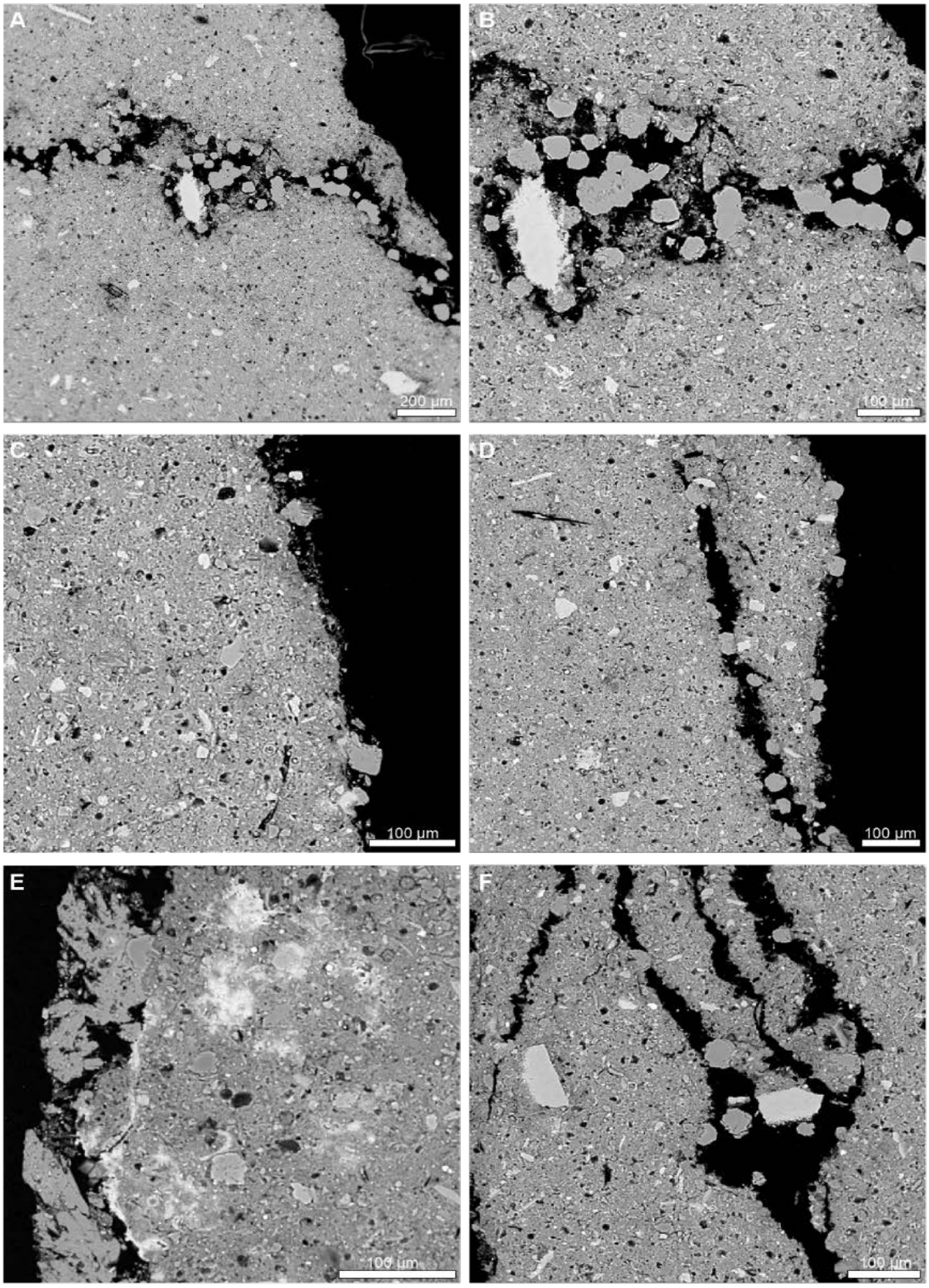

Figure F-1. EBS-14. Electron microprobe backscattered images of thin section. Opalinus Clay crack filled with large wairakite crystals in voids [**A, B, C, D, F**]. Within Opalinus Clay matrix itself, wairakite crystals occur less frequently [**C, E**].

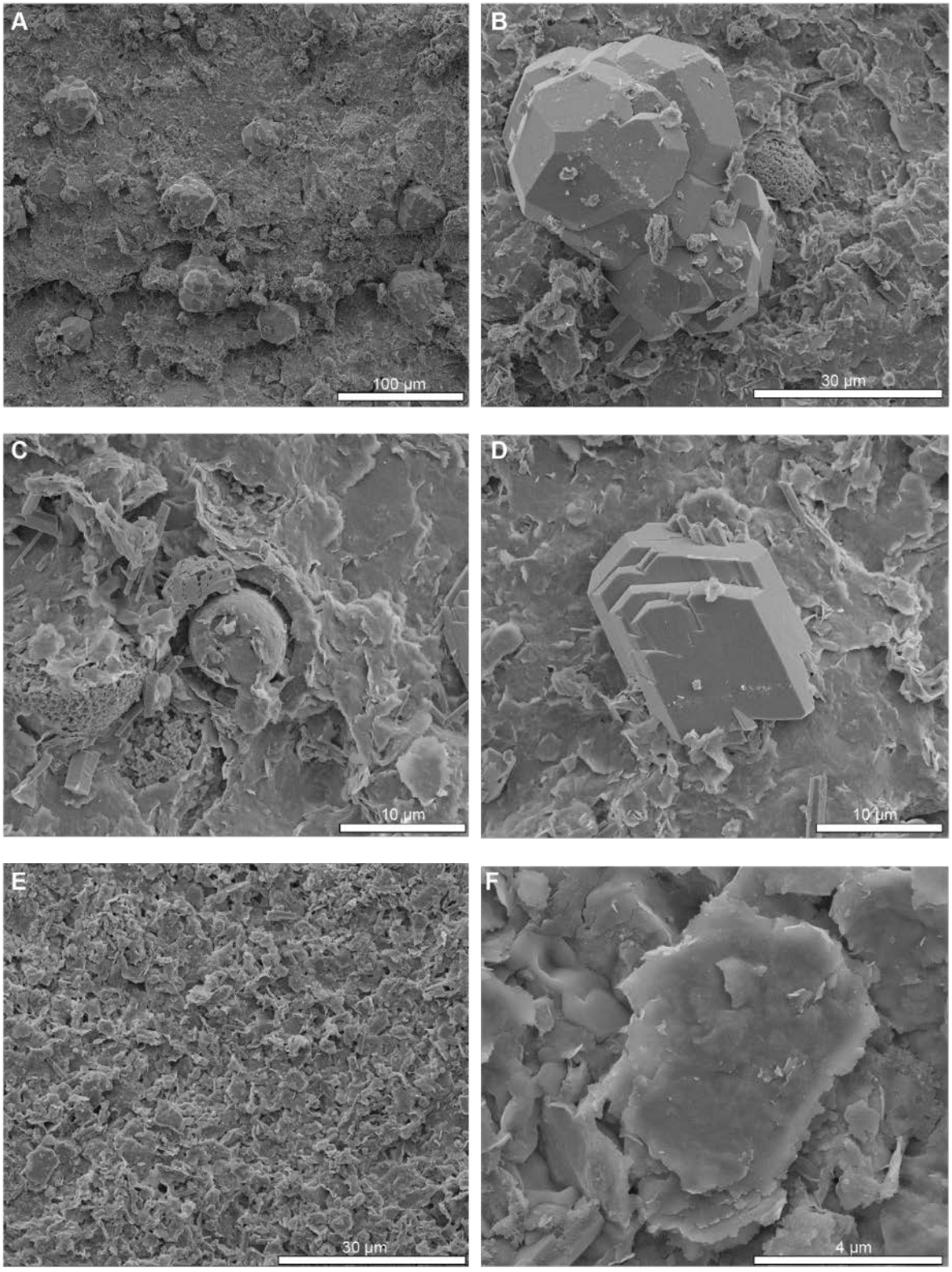

Figure F-2. EBS-14. SEM images of smectite matrix with Wairakite crystals [**A, B**] or smectite matrix alone [**E**]. Sphere of calcite [**C**] feldspar crystal [**D**] and corroded smectite [**F**].

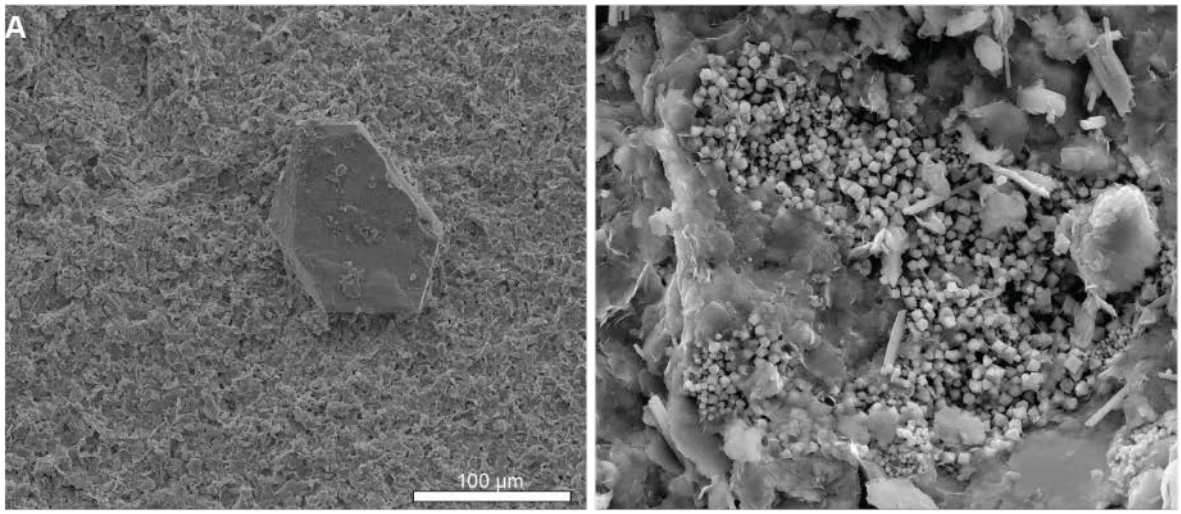

Figure F-3. EBS-14. SEM images of a carbonate imbedded in a smectite matrix [**A**] and framboidal pyrite [**B**].

SEM Images

EBS-15

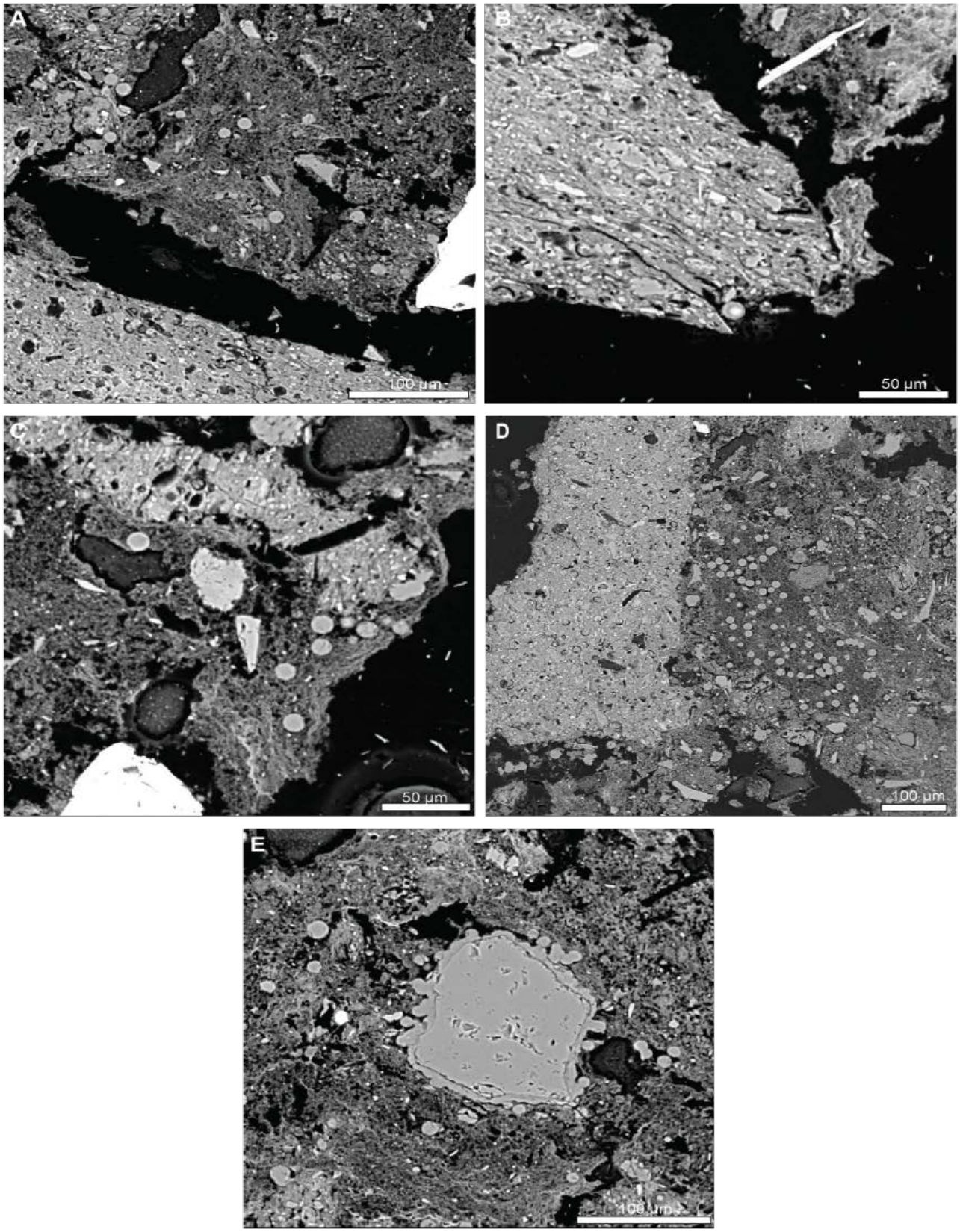

Figure F-4. EBS-15. Electron Microprobe backscattered images of Opalinus Clay with zeolites [**A, B, C**] Opalinus Clay on the left and bentonite on the right with Analcime [**D**]. Analcime mantling plagioclase [**E**].

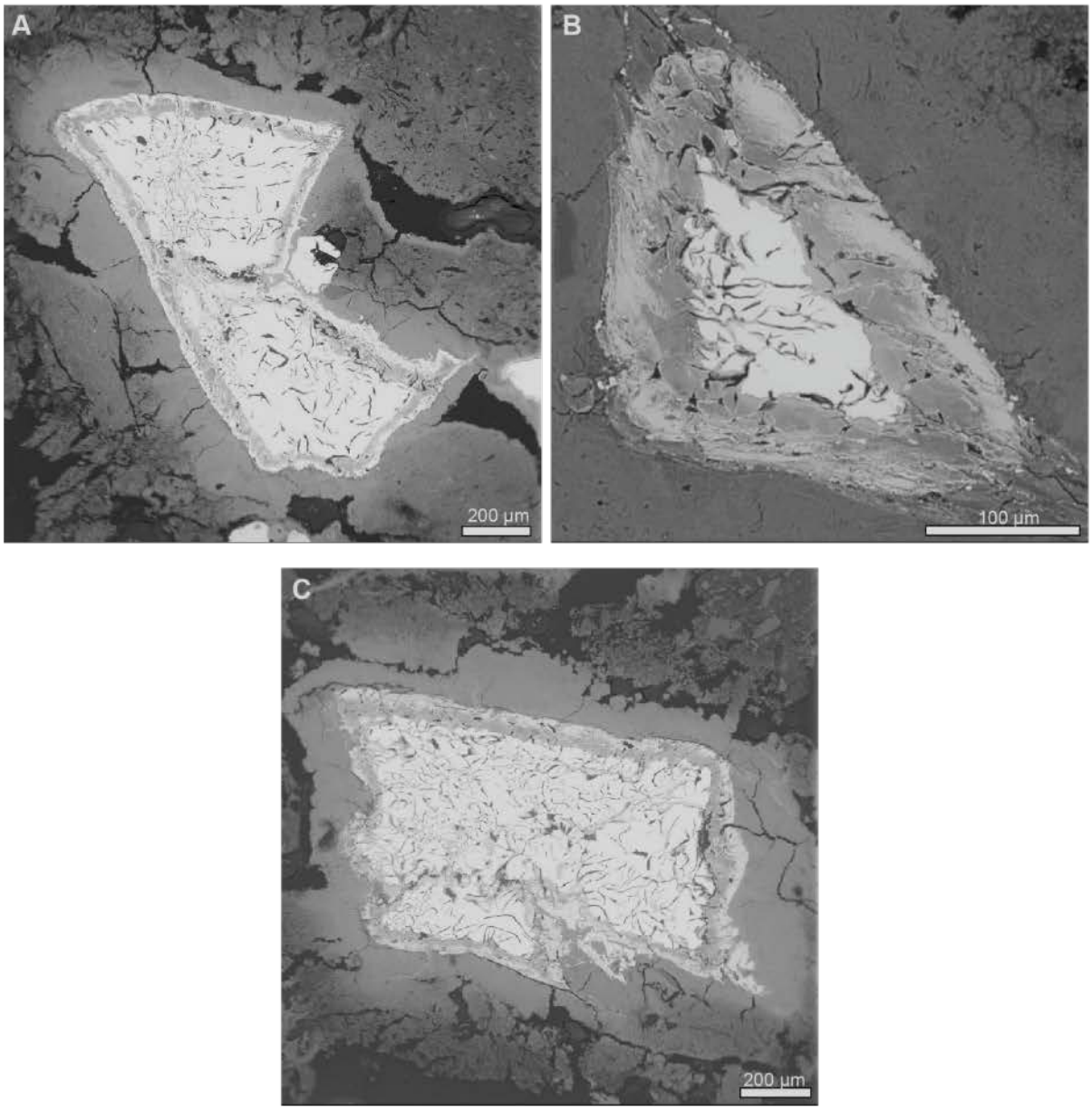

Figure F-5. EBS-15. Electron microprobe backscattered images of native iron grain with zoning and outward alteration from Fe-oxide, Fe-sulfide, stilpnomelane [**A, B, C**].

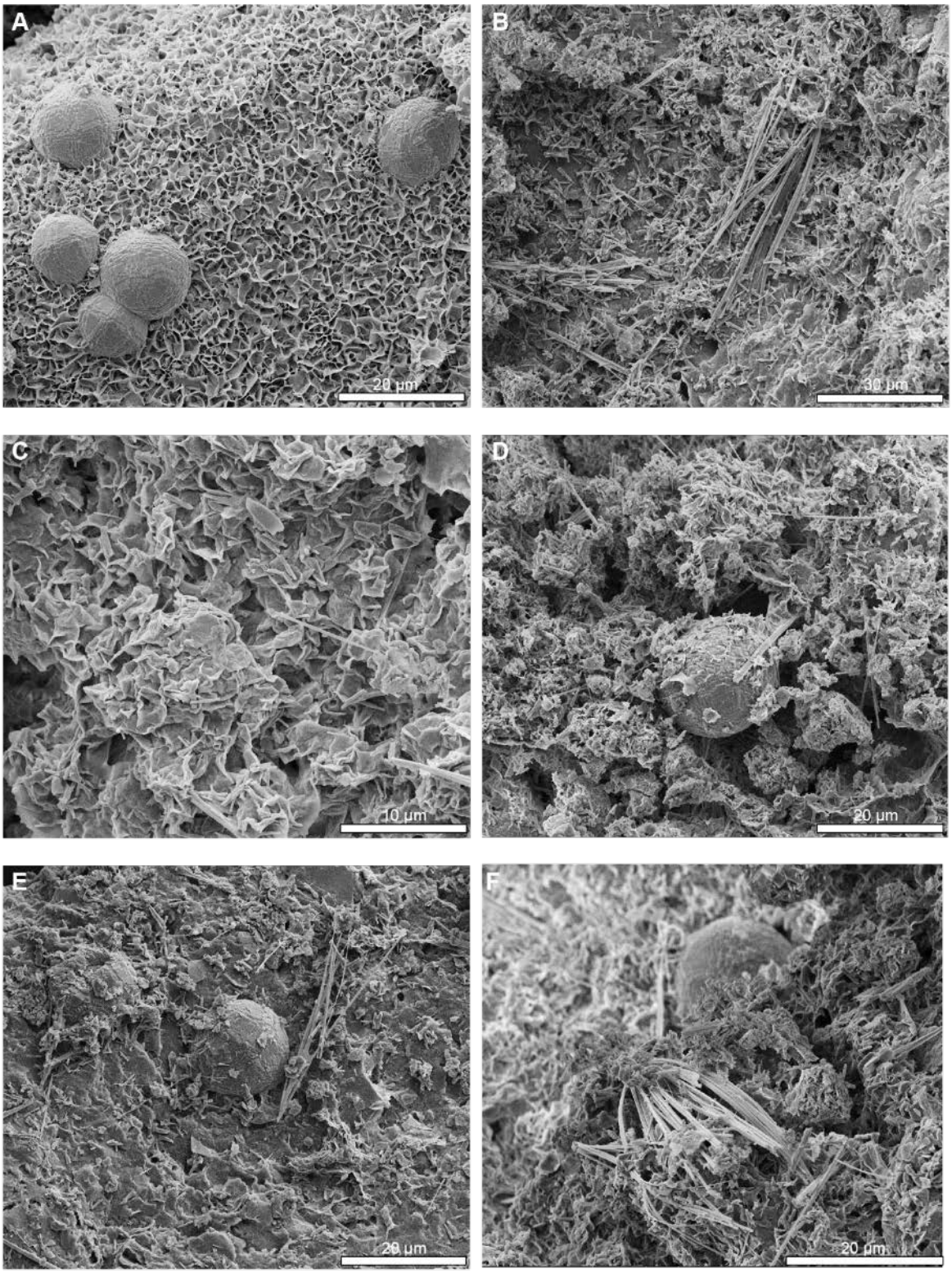

Figure F-6. EBS-15. SEM images of smectite matrix with Analcime-Wairakite crystals [**A**] illite growth [**B, F**]. Foliated bentonite with some minor illite [**C**] Analcime-Wairakite solid solution crystal with smectite and illite [**D, E**].

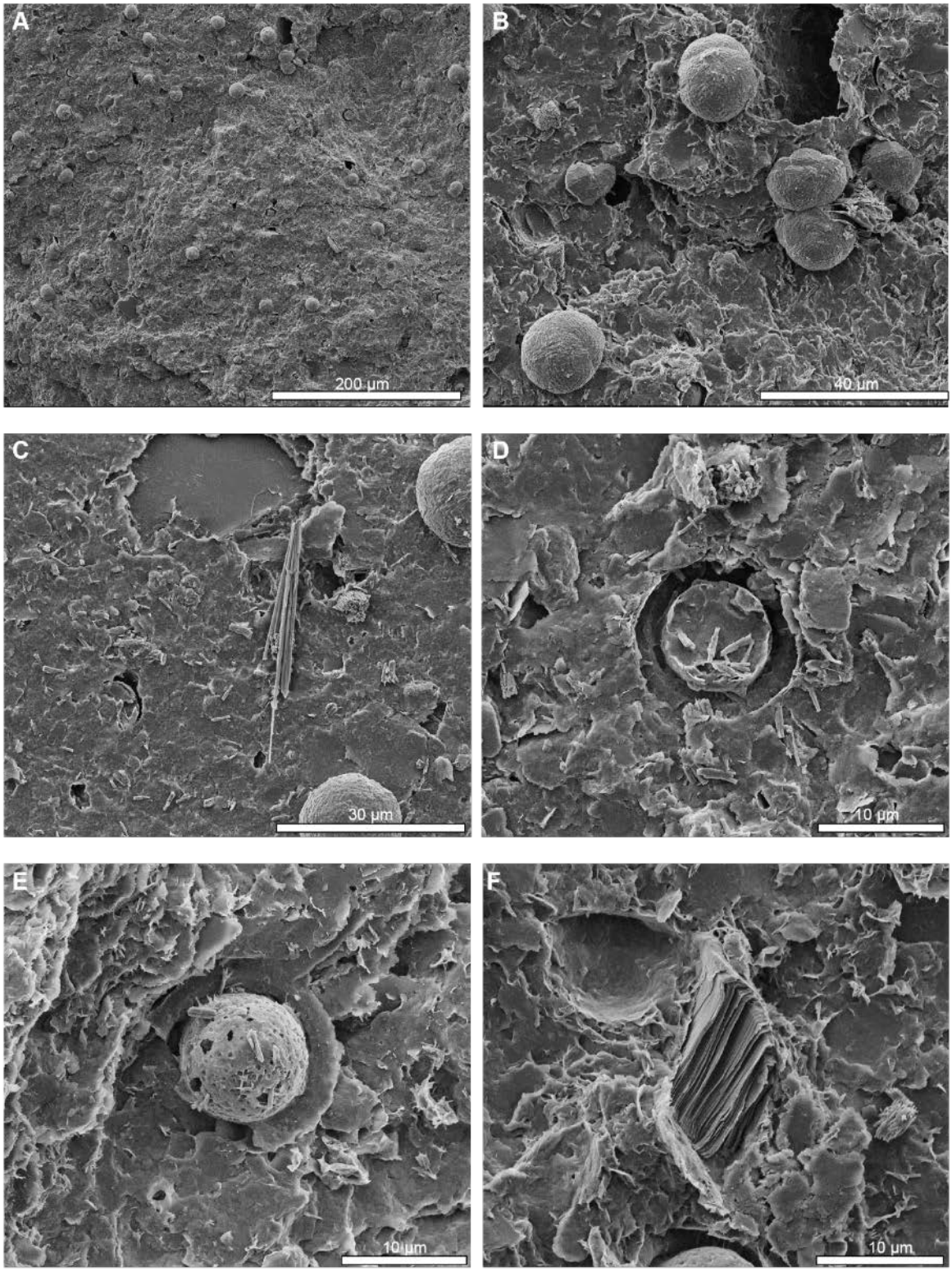

Figure F-7. EBS-15. SEM images of smectite matrix with Analcime-Wairakite crystals [**A**]. Analcime Wairakite solid solution crystals [**B**]. Possible illite [**C**] fossil cast [**D**]. Calcite ball [**E**]. Biotite [**F**].

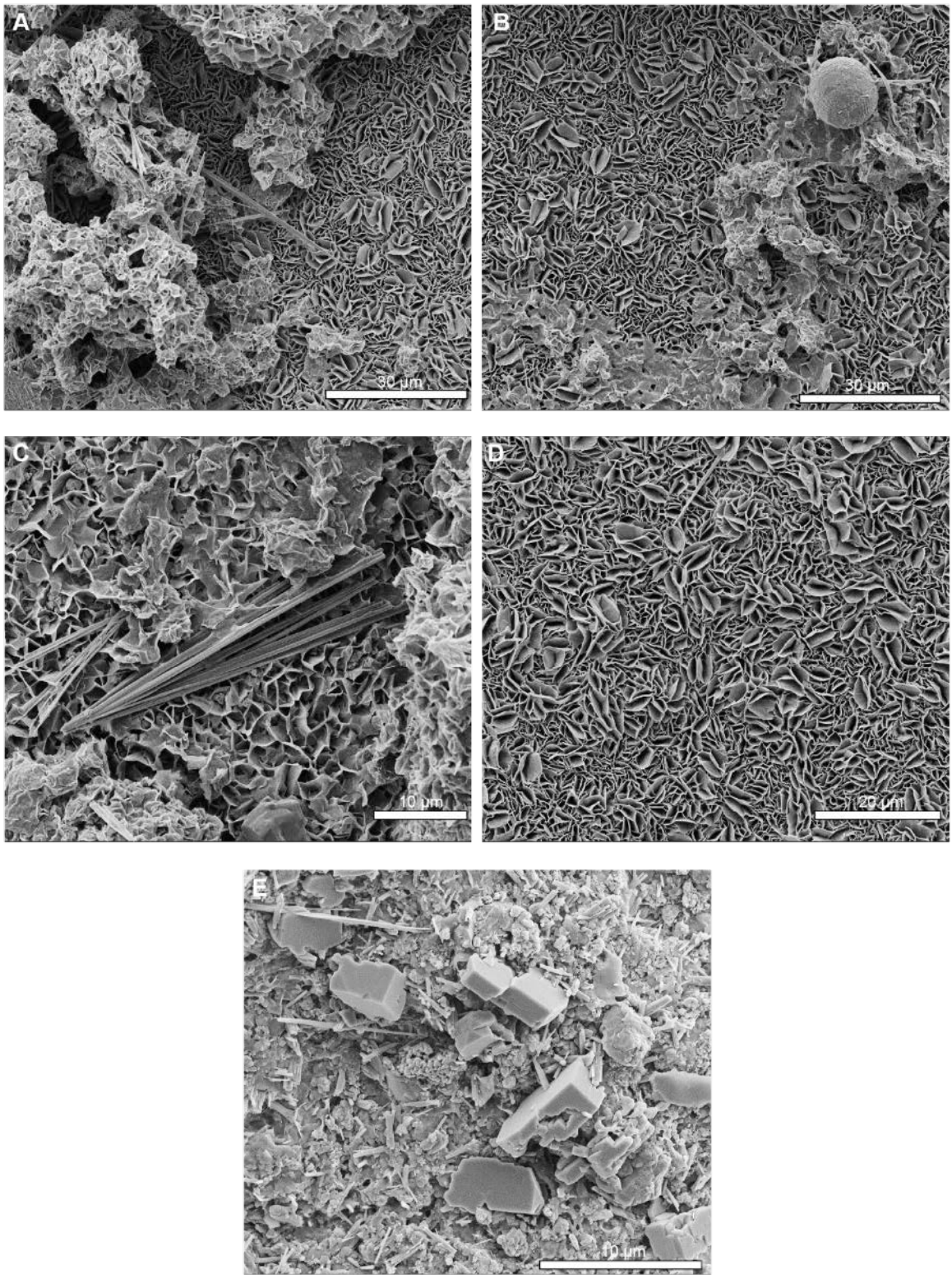

Figure F-8. EBS-15. SEM images of unknown fibrous material on saponite [**A**]. Saponite and Analcime-Wairakite crystals on 316 SS [**B**]. Fibrous millerite on saponite [**C**]. Saponite mat [**D**]. SEM image of unknown crystal growth (possibly feldspar) suspended in smectite [**E**].

SEM Images

EBS-17

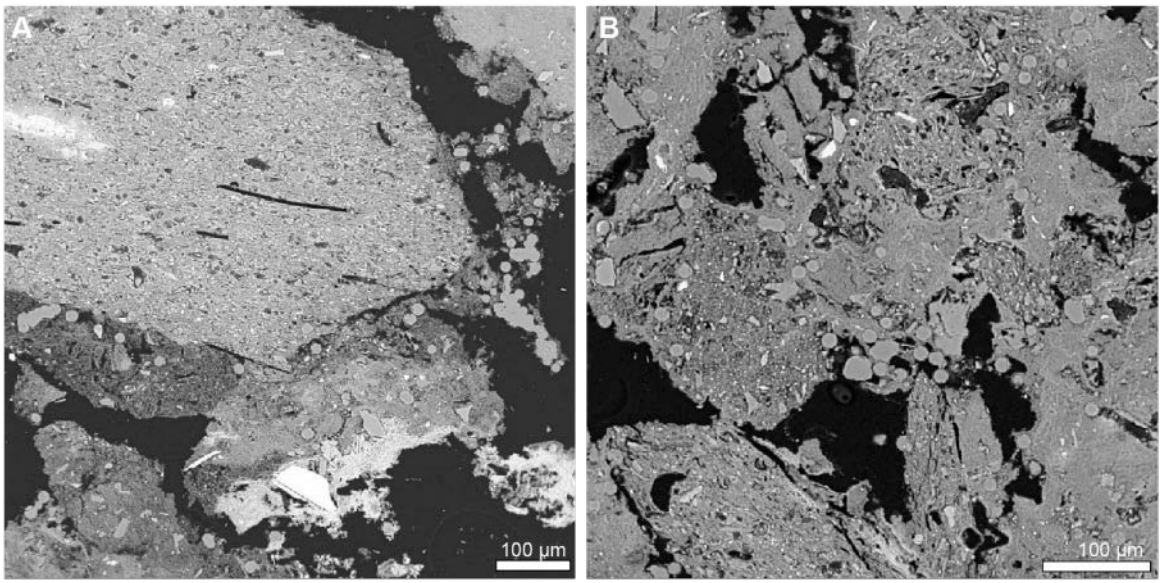

Figure F-9. EBS-17. Electron microprobe images of thin section Opalinus Clay with Analcime-Wairakite crystals [**A, B**].

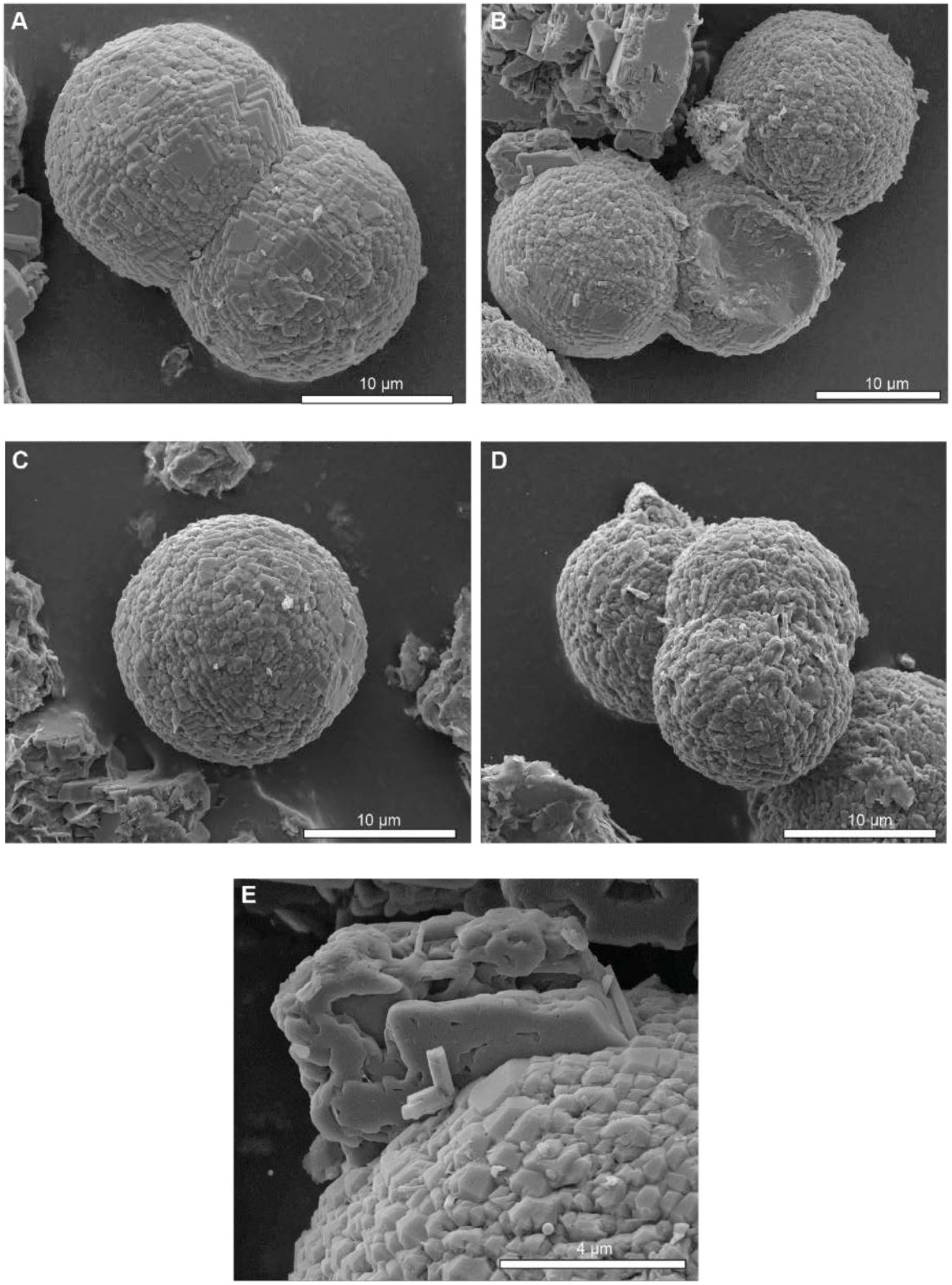

Figure F-10. EBS-17. SEM images of Analcime-Wairakite solid solution crystals [**A, B, C, D**]. Feldspar dissolution in contact with Analcime-Wairakite crystal [**E**].

SEM Images

EBS-18

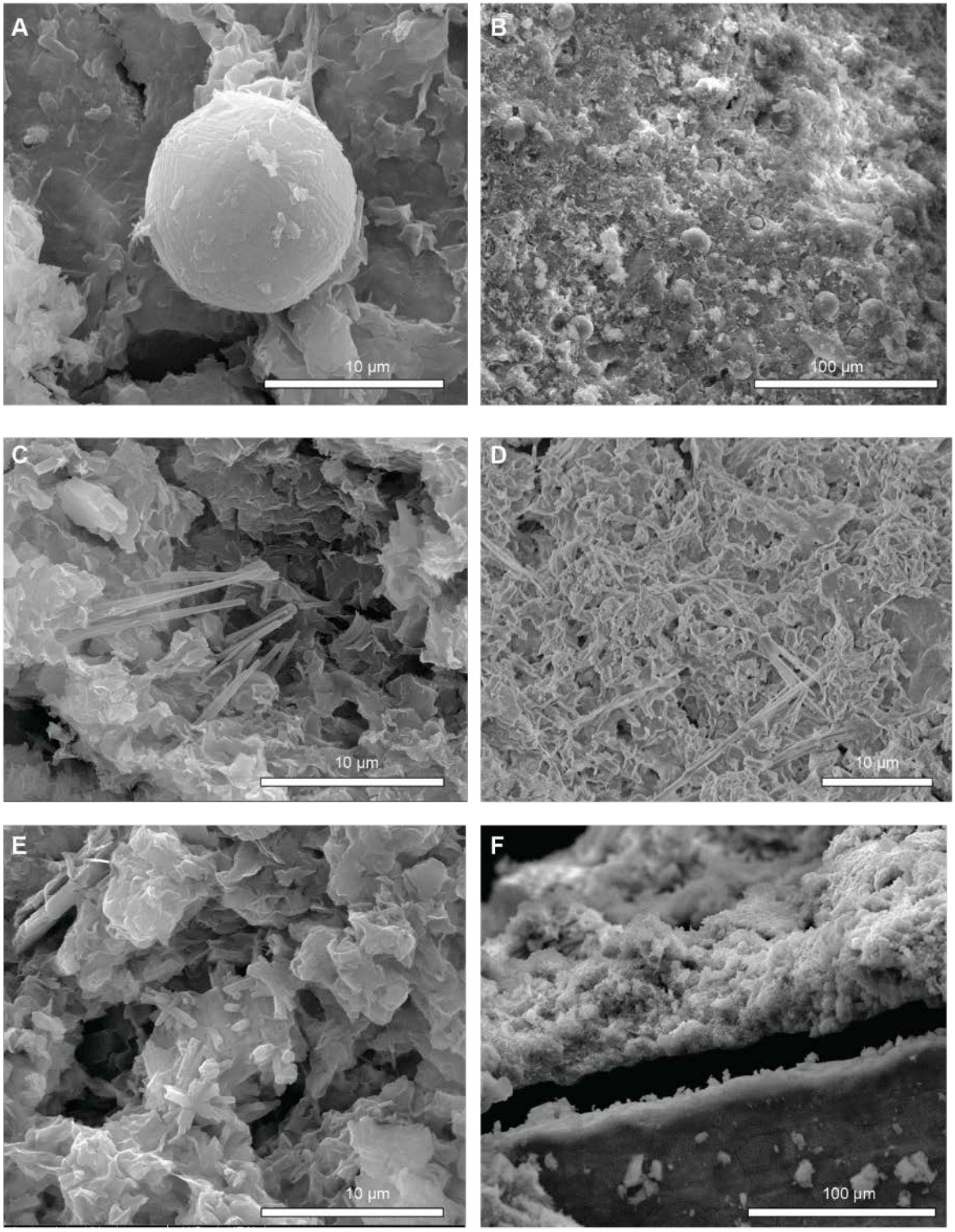

Figure F-11. EBS-18. SEM images of Analcime-Wairakite zeolite in smectite matrix [**A, B**]. Acicular [**C**] and fibrous [**D**] clinoptilolite in smectite. Radial authigenic plagioclase growth [**E**]. Fe-saponite (fine-grained material above black zone) grown on low carbon steel (lower grey mass) [**F**].

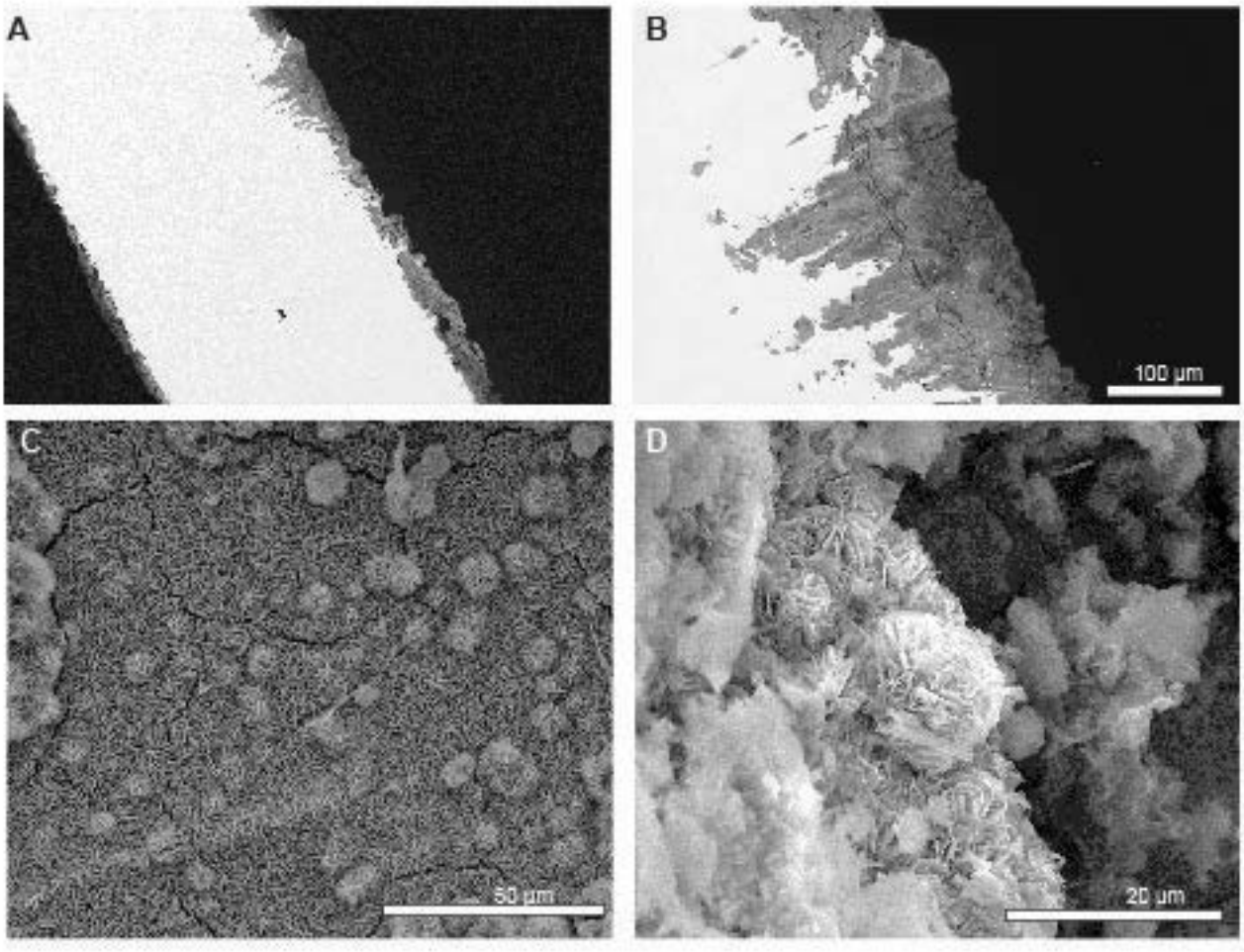

Figure F-12. EBS-18. Electron microprobe backscattered image of thin sections showing low carbon steel corrosion [**A, B**]. SEM images of Fe-saponite crystal growth perpendicular to low carbon steel [**C**] and secondary smectite rose [**D**].

SEM Images

EBS-19

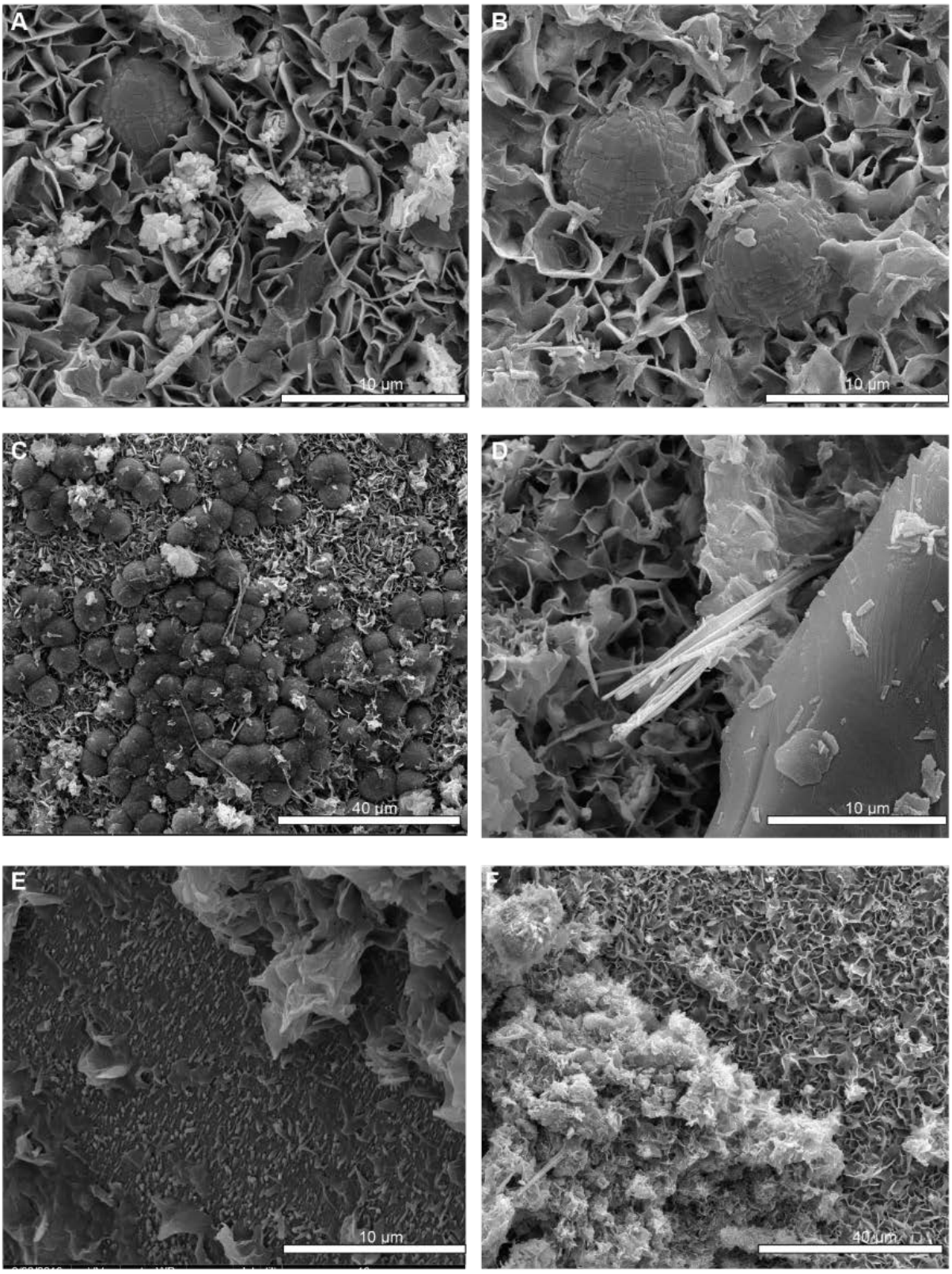

Figure F-13. EBS-19. SEM images of Fe-saponite, Analcime-Wairakite, with minor smectite, albite, and pentlandite crystals [**A**]. Analcime-Wairakite embedded in Fe-saponite [**B, C**]. In [**C**] most likely the zeolite cluster replaced glass lapilli. Acicular clinoptilolite next to resorbing K-feldspar phenocryst [**D**]. Secondary albite growth on plagioclase phenocryst [**E**] Smectite overlying Fe-saponite [**F**].

SEM Images

EBS-20

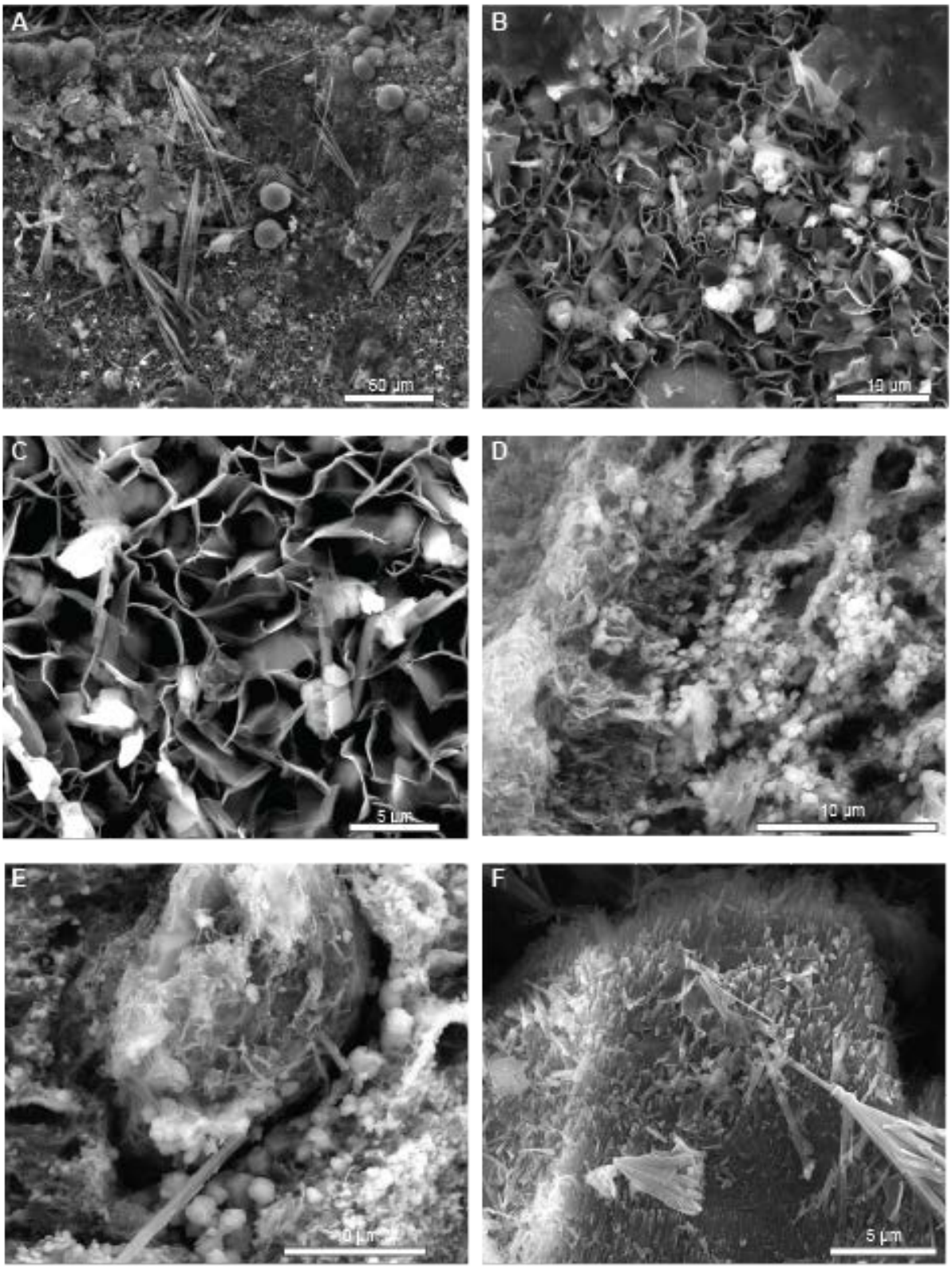

Figure F-14. EBS-20. SEM images of chlorite sprays with Analcime-Wairakite solid solution zeolite [**A, B**]. Analcime-Wairakite solid solution zeolite surrounded by Fe-saponite, with late stage pentlandite (white crystals) [**B**]. Close up of late stage pentlandite (white crystals) on Fe-saponite [**C**]. Possible calcite spheres in smectite [**D, E**]. Feldspar sprays (likely Labradorite), with background K-feldspar dissolution texture [**F**].

SEM Images

EBS-21

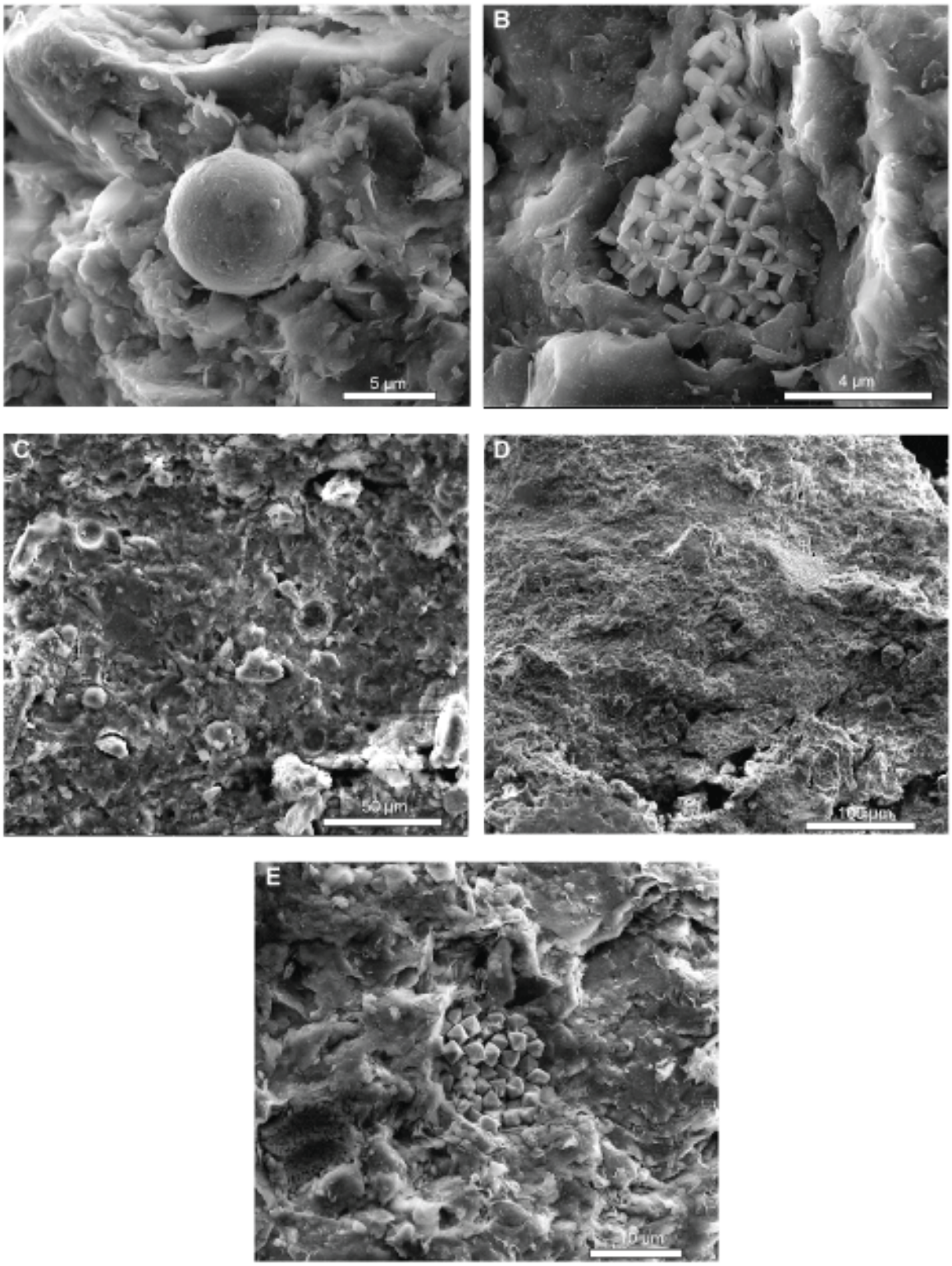

Figure F-15. EBS-21. SEM images of unknown Al-silicate in smectite matrix [**A, B**]. Examples of smectite matrix [**C, D**] and framboidal pyrite [**E**].

SEM Images

EBS-22

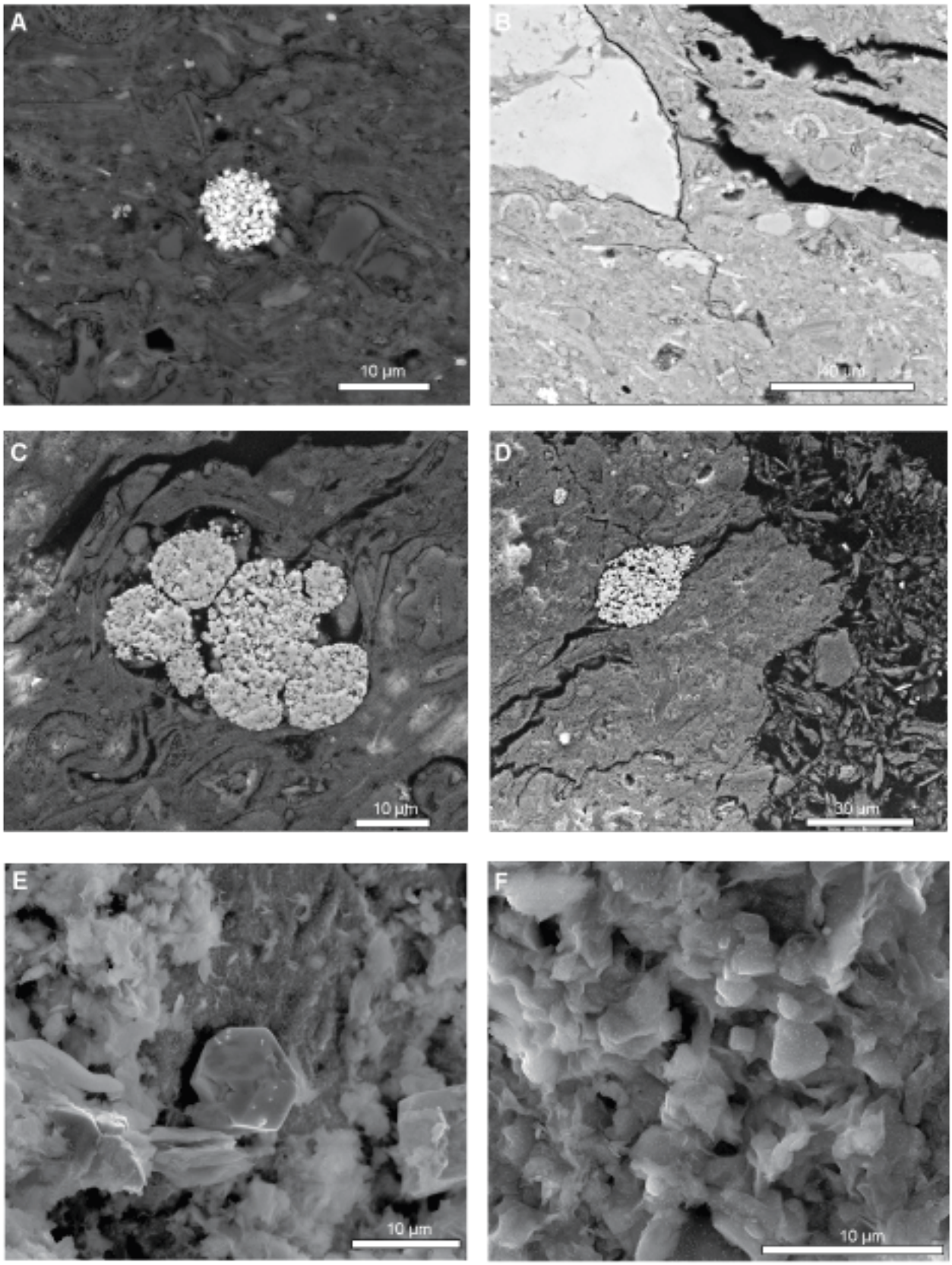

Figure F-16. EBS-22. Electron Microprobe backscattered images of framboidal pyrite [**A**] and Opalinus Clay fragments [**B, D**] with replacement of fossil casts lined with calcite [**B**] and carbonate crystal clusters [**C**]. Magnetite crystal (solid buffer material) [**E**] and authigenic quartz in center of image [**F**].

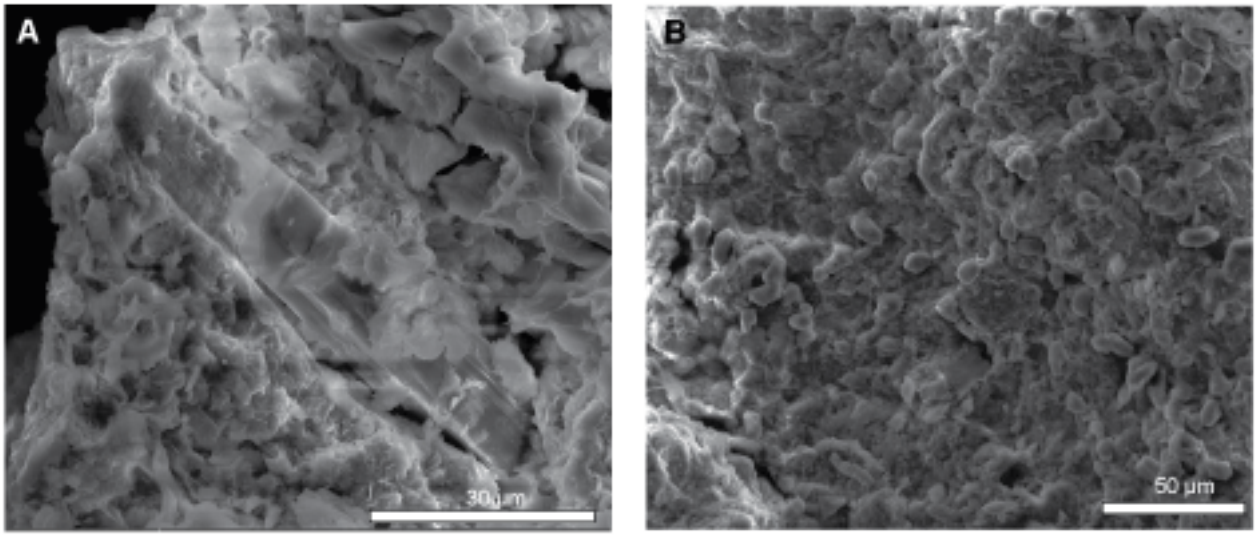

Figure F-17. EBS-22. Electron Microprobe backscattered images of secondary calcite on smectite [**A**] and authigenic gypsum lath [**B**].

SEM Images

EBS-23

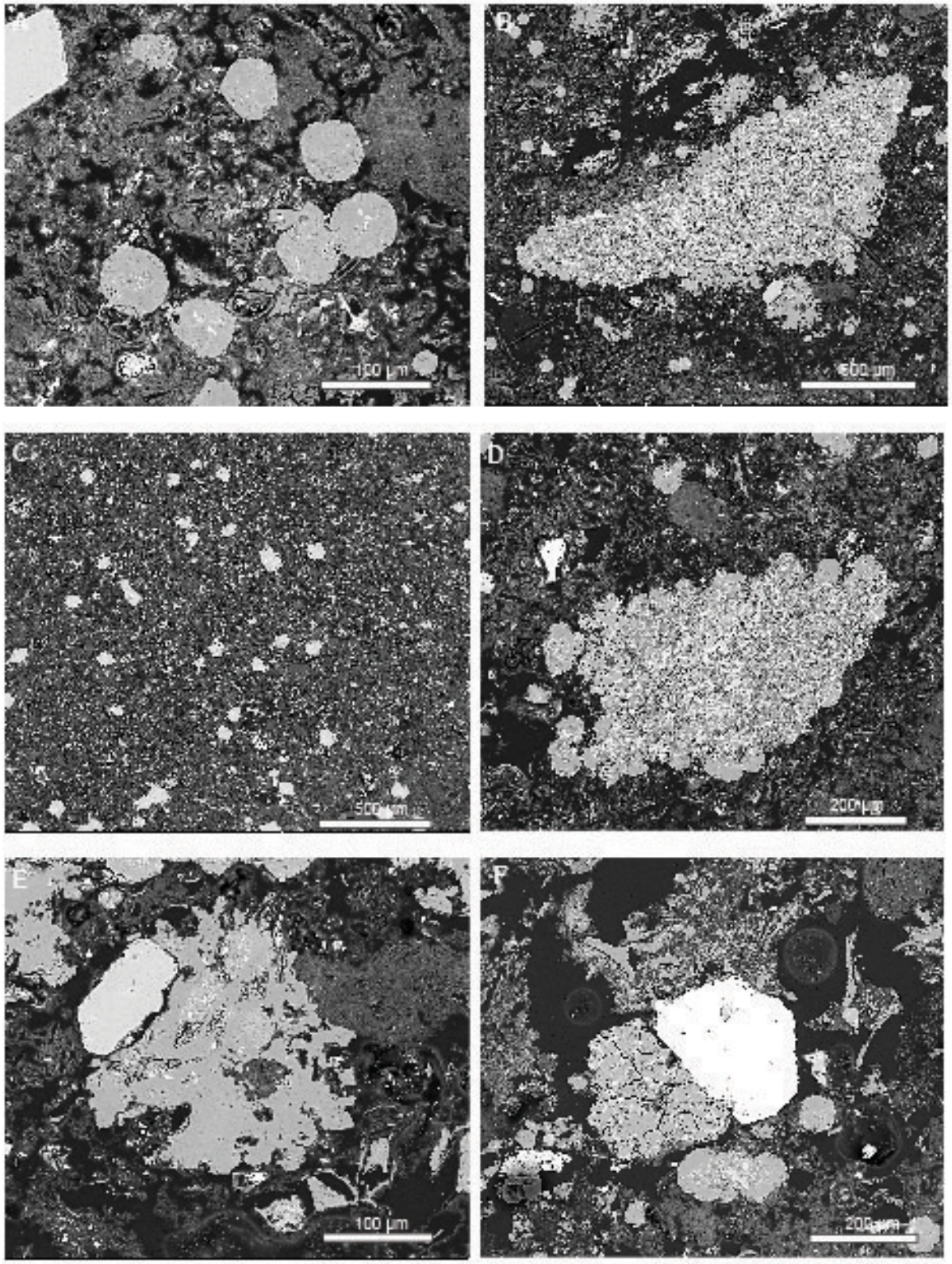

Figure F-18. EBS-23. Electron Microprobe backscattered images of Analcime-Wairakite solid solution crystals [**A, B, C**]. Note Analcime-Wairakite solid solution rims Opalinus Clay fragment [**B**]. Wairakite crystals mantling Opalinus Clay fragment [**D**]. Feldspar crystal adjacent to Analcime-Wairakite solid solution crystals replacing pumice lapilli [**E**]. Bright Fe-oxide crystal next to a Wairakite-rich analcime zeolite [**F**].

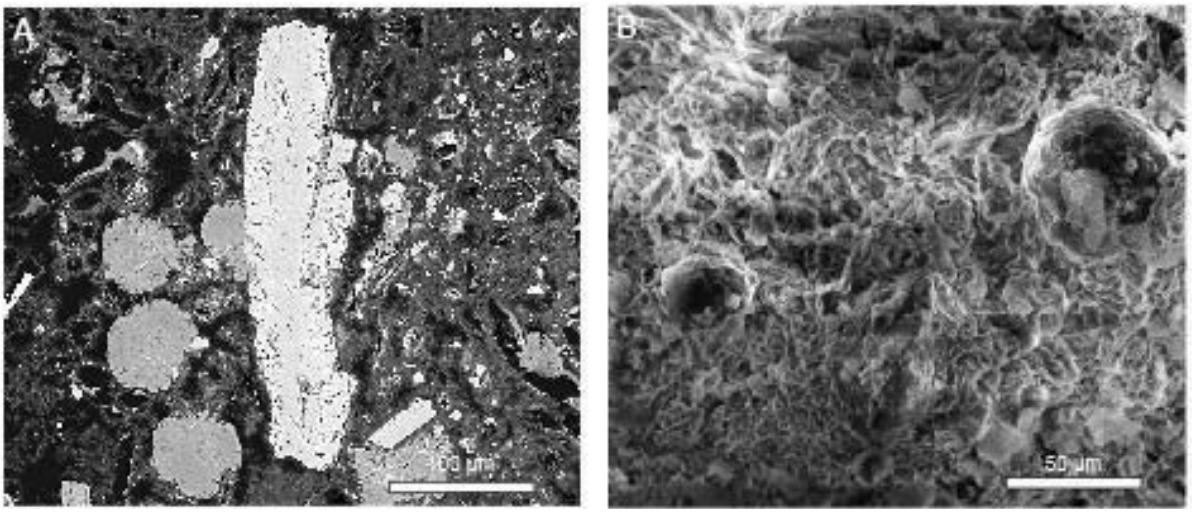

Figure F-19. EBS-23. Electron Microprobe backscattered image of calcite crystal surrounded by Analcime-Wairakite crystals. Zeolite crystals to left of calcite crystal and analcime-rich, while zeolite abutting calcite is Wairakite-rich [**A**]. Analcime-Wairakite solid solution crystals residing in smectite matrix [**B**].

FEBEX
SEM Images

INNER RING:

SAMPLES
BM-C-49-1
BM-C-49-3

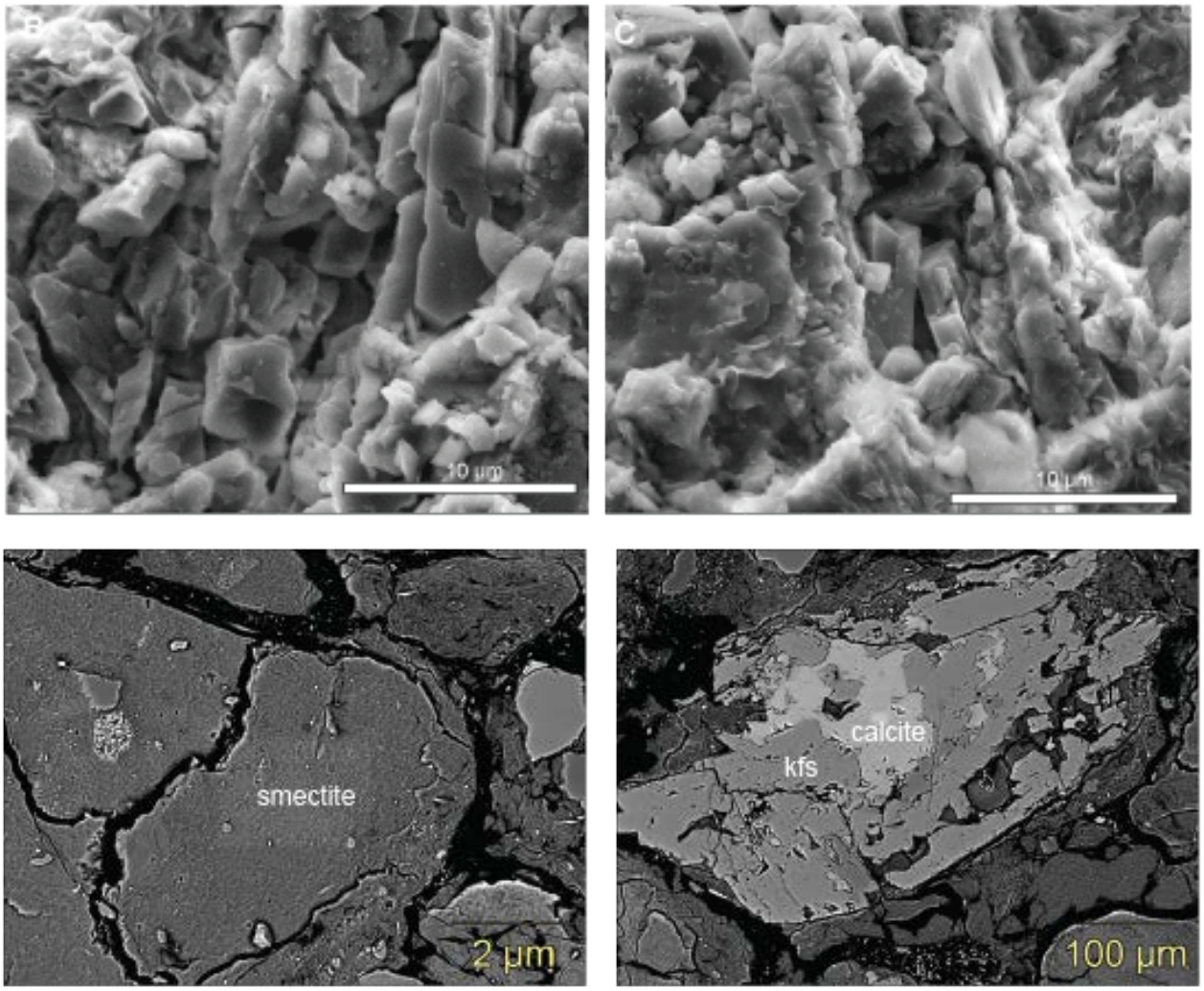

Figure F-20. FEBEX BM-C-49-1. [A, B] Electron microprobe secondary electron (SE) images of potassium feldspar/smectite mix. [C, D] Electron microprobe backscattered electron (BSE) images collected during microprobe analyses. [C] Smectite textures and morphology. [D] Intergrowth of K-feldspar (kfs) and calcite rimmed by smectite.

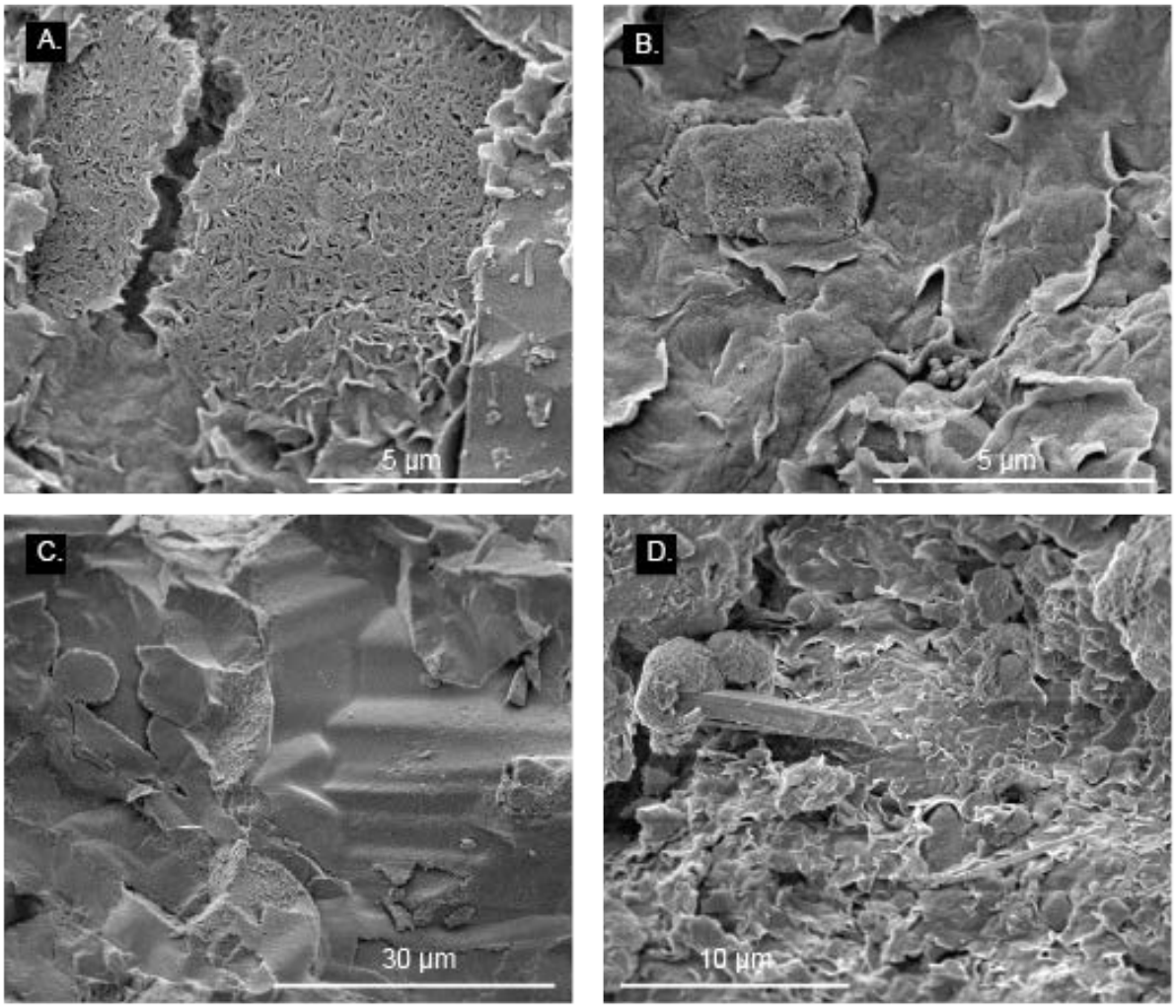

Figure F-21. FEBEX BM-C-49-3. [A, B, C, D] Electron microprobe secondary electron (SE) images depicting clay textures. [C, D] Intergrowth of plagioclase feldspar with clay.

MIDDLE RING:

SAMPLES

B-C-49-8

B-C-49-10

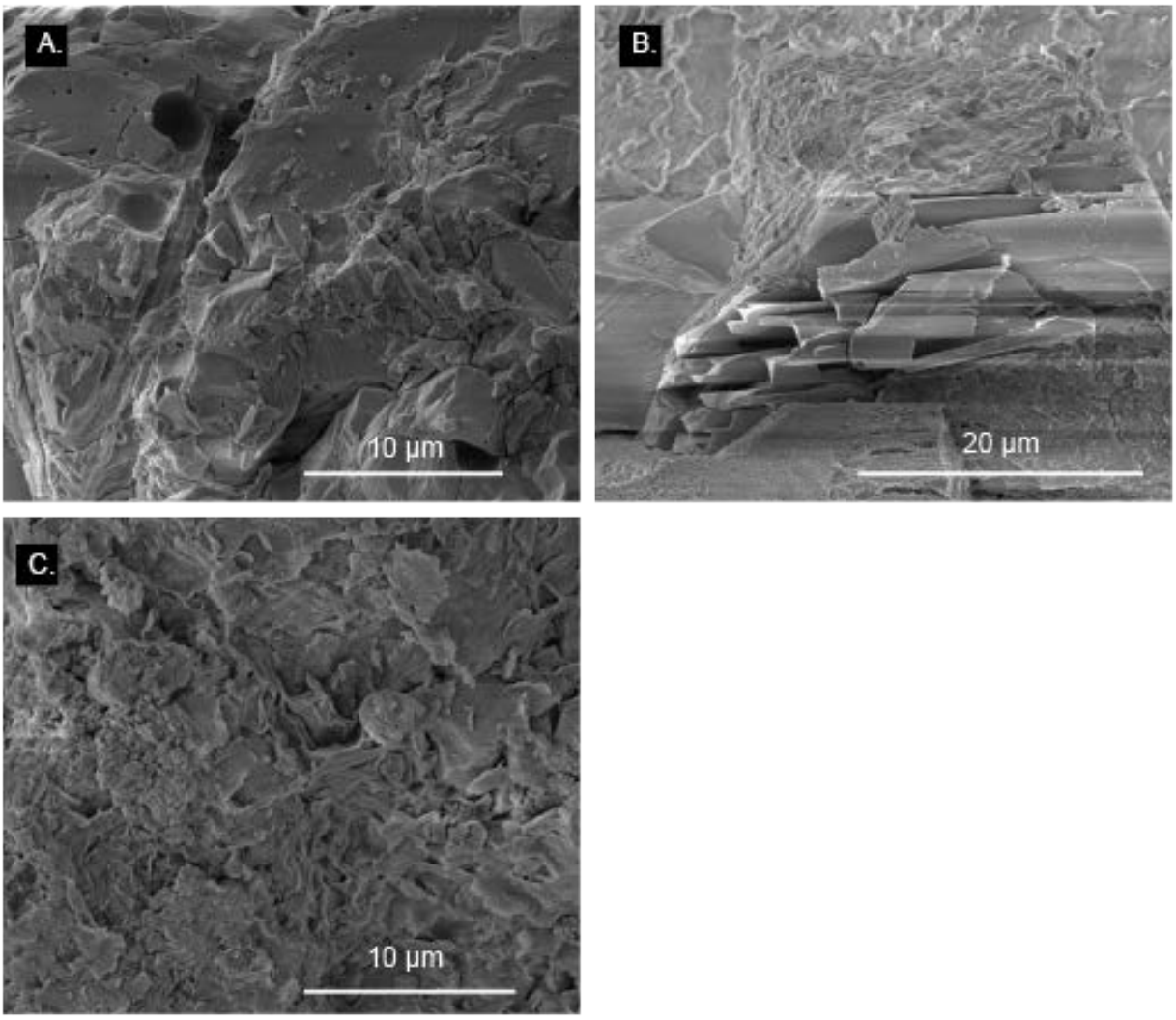

Figure F-22. FEBEX B-C-49-8. [A, B, C] Electron microprobe secondary electron (SE) images depicting clay textures and authigenic plagioclase [A, B].

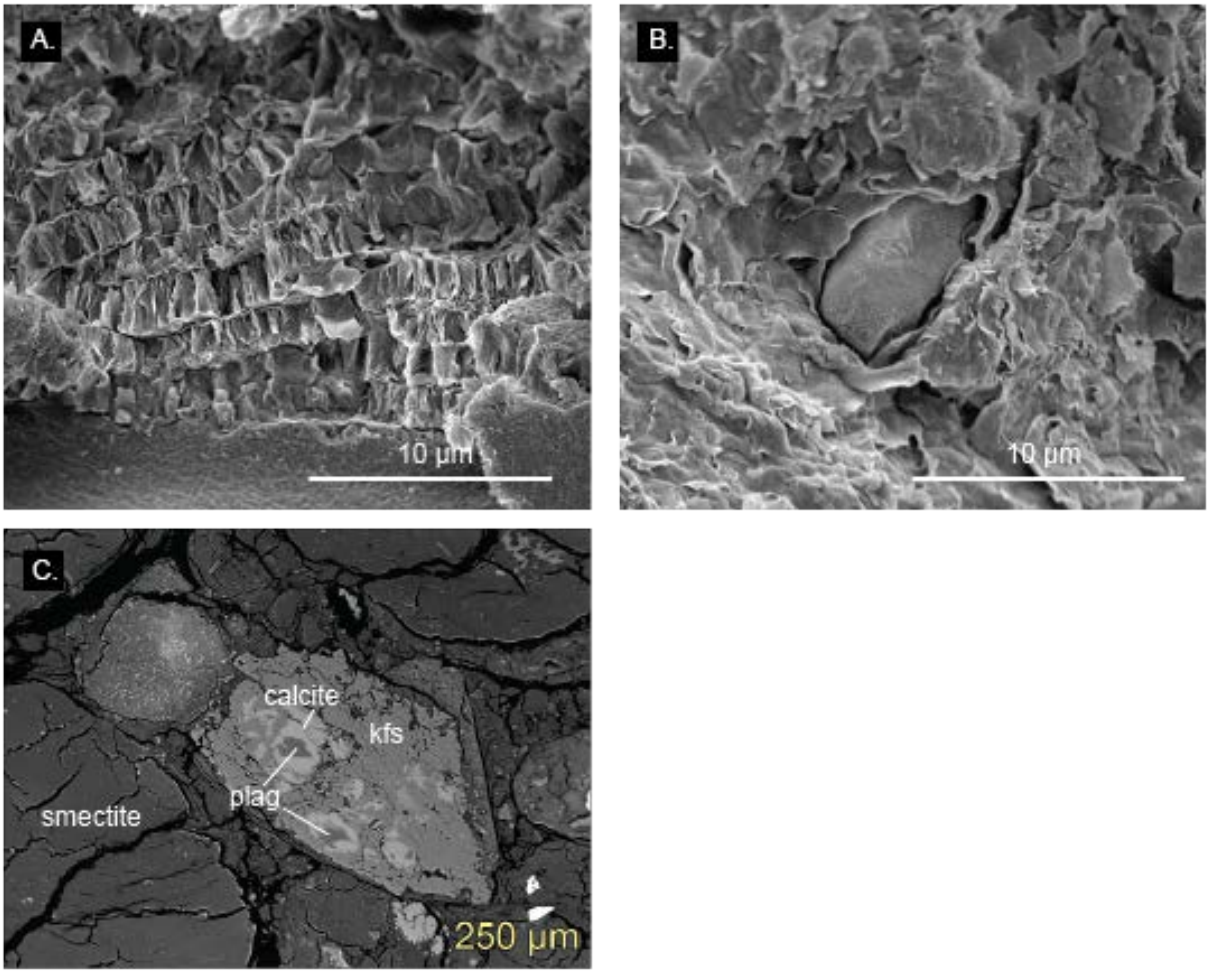

Figure F-23. FEBEX B-C-49-10. [A, B] Electron microprobe secondary electron (SE) images depicting clay textures. [C] Intergrowth of plagioclase, calcite, and K-feldspar in a smectite matrix.

OUTER RING:

SAMPLES

B-C-49-9

B-C-49-11

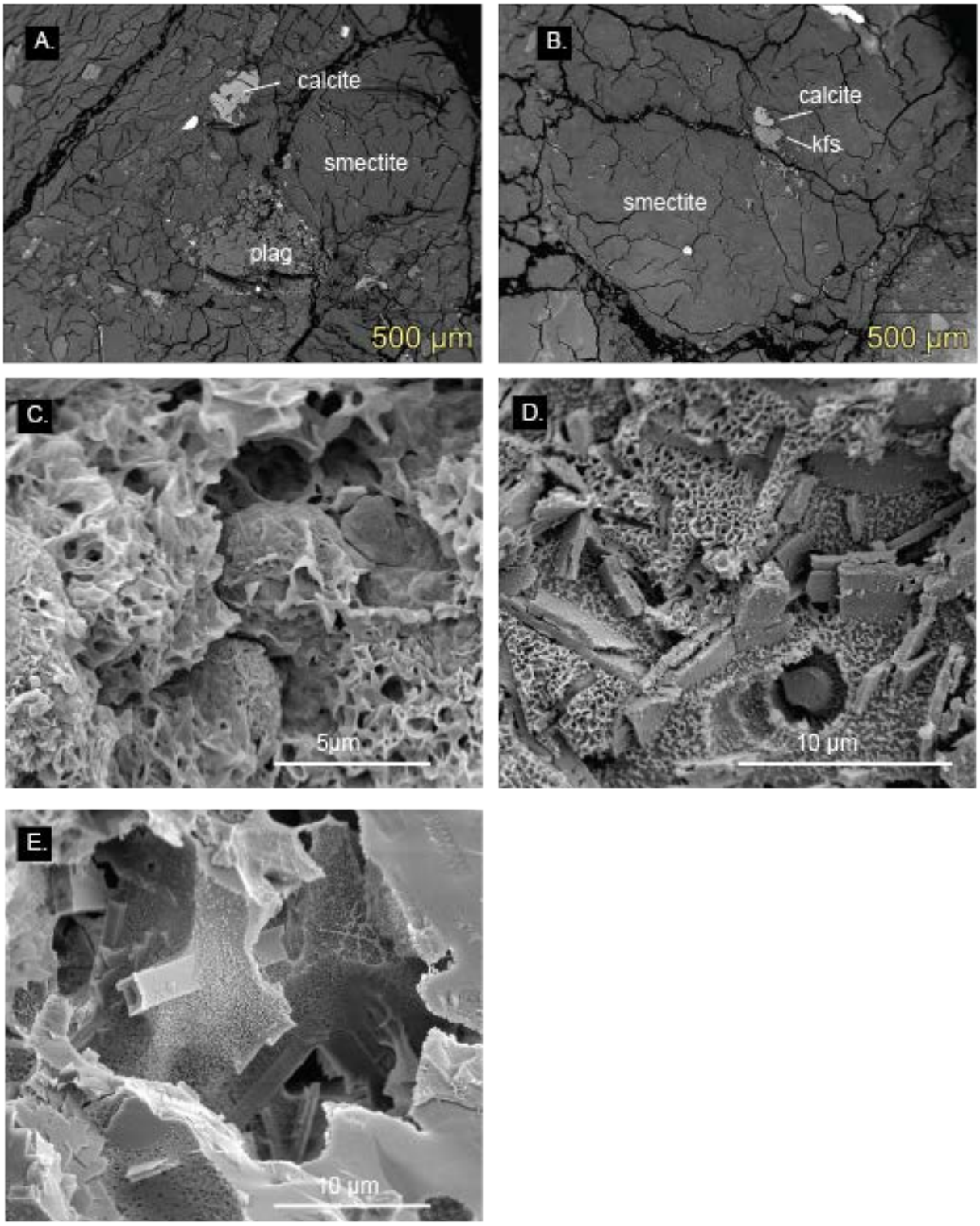

Figure F-24. FEBEX B-C-49-9. [A, B] Electron microprobe BSE images. [C, D, E] SE images of clay matrix and authigenic blocky, elongate feldspar crystals [D, E].

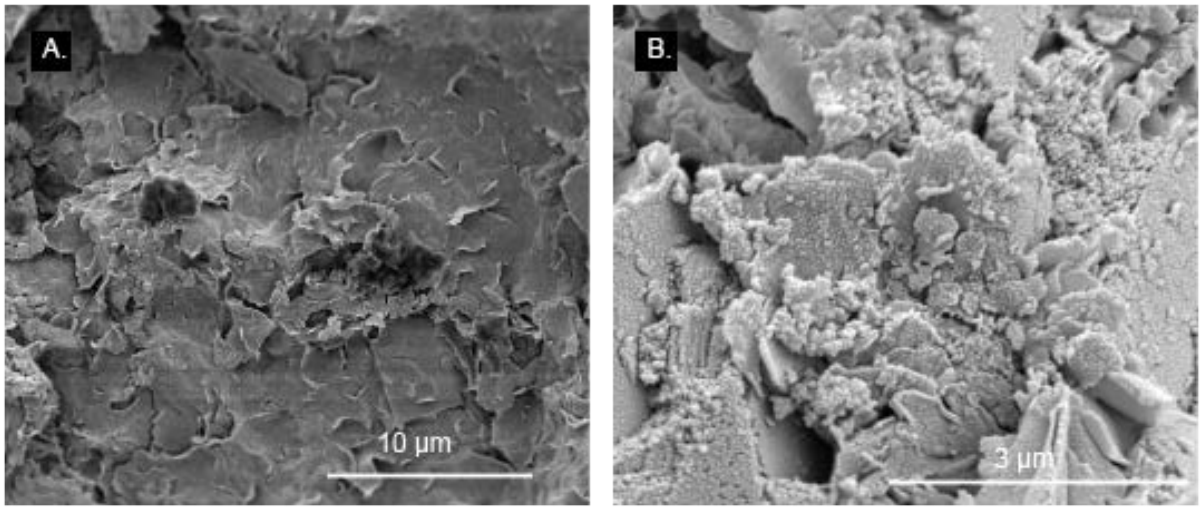

Figure F-25. FEBEX B-C-49-11. [A, B] Electron microprobe SE images. [A] Clay texture. [B] Authigenic albite growth.